RESEARCH ARTICLE

VOLCANICA

What lies beneath the ice? Using the geochemistry and geochronology of modern river cobbles to better decipher the evolution of a glaciated volcanic arc (Wrangell Arc, Alaska, U.S.A.)

Matthew Brueseke*[α], Beth K. Morter[α], Jeffrey A. Benowitz[β], Jeffrey M. Trop[γ], Stanley A. Mertzman[δ], Carl S. Kirby[γ], and Kailyn Davis[ε]

[α] Department of Geology, Kansas State University, 108 Thompson Hall, Manhattan, KS 66506, USA.
[β] GeoSep Services, 1521 Pine Cone Road, Moscow, ID, 83843, USA.
[γ] Department of Geology & Environmental Sciences, Bucknell University, Lewisburg, PA 17837, USA.
[δ] Department of Earth and Environment, Franklin and Marshall College, Lancaster, PA 17604, USA.
[ε] Geophysical Institute and Geochronology Laboratory, University of Alaska Fairbanks, Fairbanks, AK 99775, USA.

Abstract

The ~30 Ma to Recent Wrangell Arc, Alaska, is an ideal location to study subduction and slab-edge magmatism. However, the Wrangell Arc covers a huge area (~15,000 km^2) and ~29 % of the Wrangell Arc is covered by glaciers with rugged topography, making bedrock sampling challenging. We addressed these barriers with geochemical and geochronologic analyses on igneous cobbles collected from rivers encircling the Wrangell Arc. Results show that magmatism migrated southward and then northwestward, mirroring bedrock studies. Cobble geochemistry overlaps bedrock results, where calc-alkaline and adakitic cobbles are spatially and temporally ubiquitous in the Wrangell Arc, indicating that subduction and slab melting have been dominant processes throughout the entire ~30 myr duration of the volcanic arc. Intra-arc extension–related transitional-tholeiitic cobbles are not found in southwestern Wrangell Arc rivers and are spatially and temporally limited in both bedrock and cobble data. The novel method we describe here closely replicates the bedrock record in geochemical, temporal, and spatial contexts and can be used when there are bedrock access concerns and/or for characterizing watersheds.

Non-technical summary

Bedrock sampling over large regions (~1000 km^2) is challenging due to time and cost constraints and is especially problematic when large parts of those regions are covered by glacial ice, limiting exposure, or are generally inaccessible. Here, we demonstrate that igneous cobbles from modern river bars can be sampled, and then analyzed for age and geochemical characteristics, and be used indirectly to sample bedrock exposed upslope in the sampled watershed. This approach allows for more efficient geological characterization at the scale of a volcanic arc compared with conventional bedrock sampling. This combined geochemical-geochronological detrital cobble approach can be applied in other settings dominated by igneous bedrock that is dissected by active fluvial systems.

Keywords: Detrital; Clast; Igneous Petrology; Subduction Zones; Volcanic Field; Sampling.

1 Introduction

Investigations of modern river and glacial detrital sediment to characterize the entirety of a watershed's bedrock magmatic history have until recently been restricted to bulk sediment geochemistry and/or single grain applications (e.g. geochronology of detrital zircons or mud geochemistry) [Clift et al. 2008; Gehrels 2012; Benowitz et al. 2019; Malkowski et al. 2019]. Applying both isotopic analysis and U-Pb geochronology on individual detrital zircon grains has also been used to capture the petrogenesis history of large magmatic belts [e.g. Barth et al. 2013]. Furthermore, investigating detritus from heavily glaciated volcanic regions can be a powerful tool because modern sediments can act as a proxy for bedrock that is inaccessible due to permanent ice cover and/or challenging terrain [Carley et al. 2017]. Sediment provenance interpretations derived solely from detrital zircon geochronology has limitations, which include the inherent population bias of felsic igneous rocks crystallized at (low) temperatures where zircon is stable and plentiful compared to mafic rock products [e.g. Dickinson 2008; Malusà et al. 2016; Spencer et al. 2018; Trop et al. 2022] and bedrock weathering and erosion differences [Amidon et al. 2005; Capaldi et al. 2017]. Furthermore, critical bulk rock composition and petrological information are unavailable when applying single grain methodologies.

The scope of detrital studies has been expanded to utilize modern river gravel to understand processes such as focused exhumation in glaciated areas by leveraging thermochronology and petrology descriptions on individual cobbles [Grabowski et al. 2013] and provenance of glacial sediments [Licht and Hemming 2017]. The sources for sedimentary deposits have been illuminated with combined geochemistry and geochronology on clasts from ancient strata (VanderLeest et al. [2020], who used N = 30 samples for geochemistry and N = 7 for geochronology). Here, we obtained geochemical and age data on cobbles longer than 10 cm to test the effectiveness of detrital cobble sampling to characterize the geochemical, temporal, and spatial evolution of a glacier-covered

* brueseke@ksu.edu

Submitted: 2023-05-09 | Accepted: 2023-07-31 | Published: 2023-09-12

Editor: L. Elkins | Typesetter: J. Farquharson

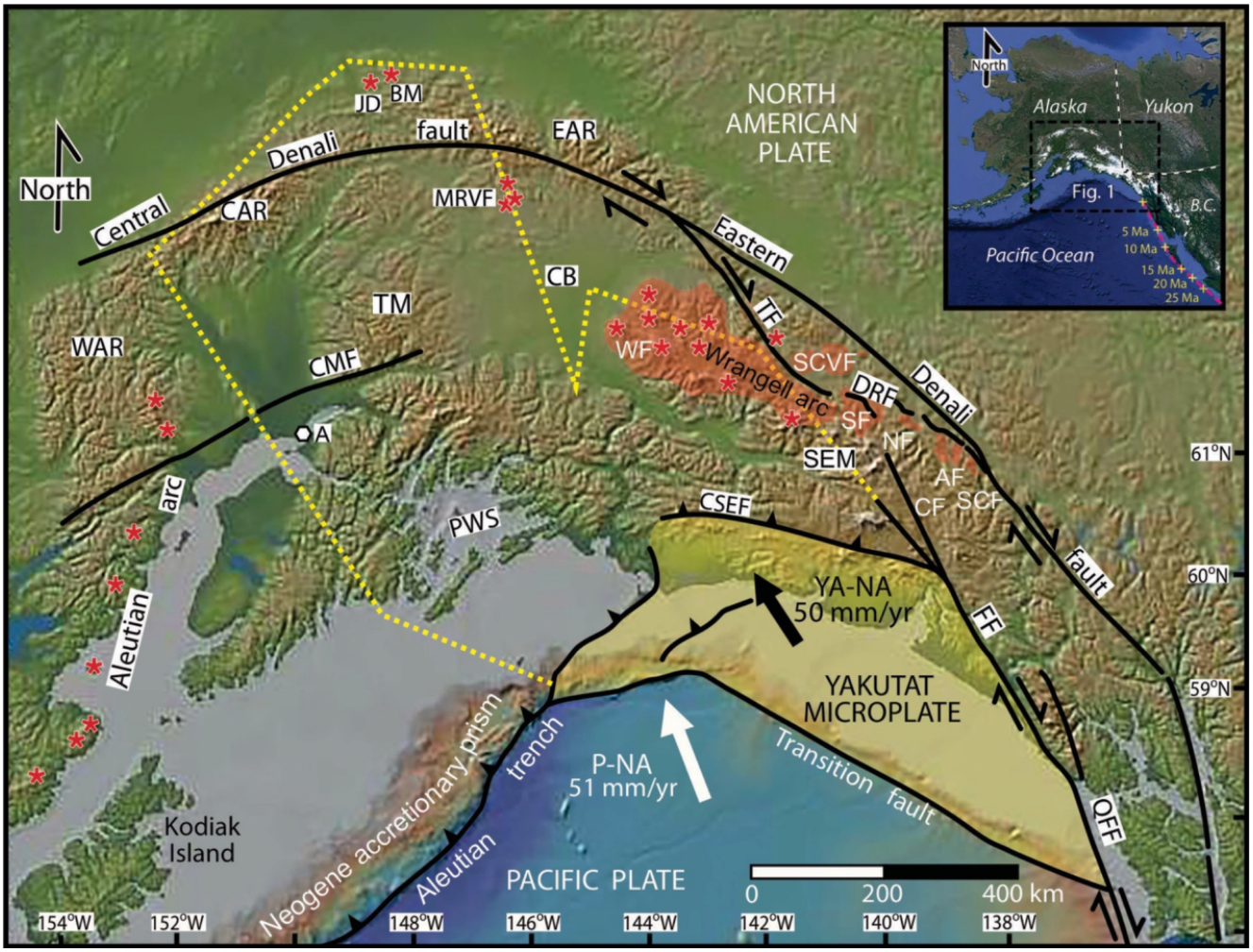

Figure 1: Map showing the tectonic framework of southern Alaska, the Yukon, and coastal British Columbia [after Trop et al. 2022]. The map shows exposed (light yellow shading, underneath Yakutat microplate label) and interpreted subducted extent (region within a bold dashed yellow line) of the Yakutat microplate, shows regional Neogene faults, and volcanic fields comprising the Wrangell Arc (transparent red, after Brueseke et al. [2019]) in Alaska (SCVF—Sonya Creek field, WF—Wrangell volcanic field) and Canada (AF—Alsek field, NF—Nines Creek field, SF—St. Clare field) including <5 Ma volcanoes denoted by red asterisks. The yellow dashed line denotes the edge of subducted Yakutat microplate [Mann et al. 2022]. The dashed magenta curve in the index map in the upper left shows Fairweather–Transition–Queen Charlotte fault intersection triple junction track during the past 25 myr [Pavlis et al. 2019]; yellow crosses show Fairweather–Transition–Queen Charlotte triple junction location at time points. Abbreviations: A—Anchorage; B.C.—British Columbia, BM—Buzzard Creek maar, CAR—central Alaska Range, CB—Copper River basin, CF—Connector fault (inferred), CMF—Castle Mountain fault, CSEF—Chugach-St. Elias fault, DRF—Duke River fault, EAR—eastern Alaska Range, FF—Fairweather fault, HCF—Hines Creek fault, JD—Jumbo Dome volcano, MRVF— Maclaren River volcanic field, QFF—Queen-Charlotte-Fairweather fault, P-NA—Pacific-North American plate, PWS—Prince William Sound, SEM—St. Elias Mountains, TM—Talkeetna Mountains, TF—Totschunda fault, WAR—western Alaska Range. Y-NA—Yakutat-North American plate.

arc compared to: 1) a conventional bedrock sampling strategy that can be hampered due to ice coverage and mountainous terrain inaccessibility, participant physical abilities, and the time-cost inefficiencies of bedrock sampling an expansive arc and 2) the standard single-grain geochronology approach that can be hampered due to mineral fertility issues and the lack of lithologic and bulk-rock geochemical information.

This study demonstrates a "test of concept" geochemistry (N = 206) and geochronology (N = 100) tandem-method (N = 100) methodology on cobbles from 17 strategically selected rivers draining the glacier-covered Wrangell Arc. The Wrangell Arc is a continental volcanic arc in south-central Alaska that is characterized by large shield volcanoes, stratovolcanoes, and cinder cones [Preece and Hart 2004; Brueseke et al. 2019], as well as ice fields, glaciers, and huge river systems (Figures 1, 2). The Wrangell Arc contains ~9,200 km^2 of volcanic and plutonic rocks in an ~15,000 to 20,000 km^2 area, with peak elevations ranging from ~700 to 5000 m [Richter et al. 1990; Trop et al. 2022]. Of this huge area, nearly ~29 % total (up to ~50 % of ice coverage in some watersheds) is covered

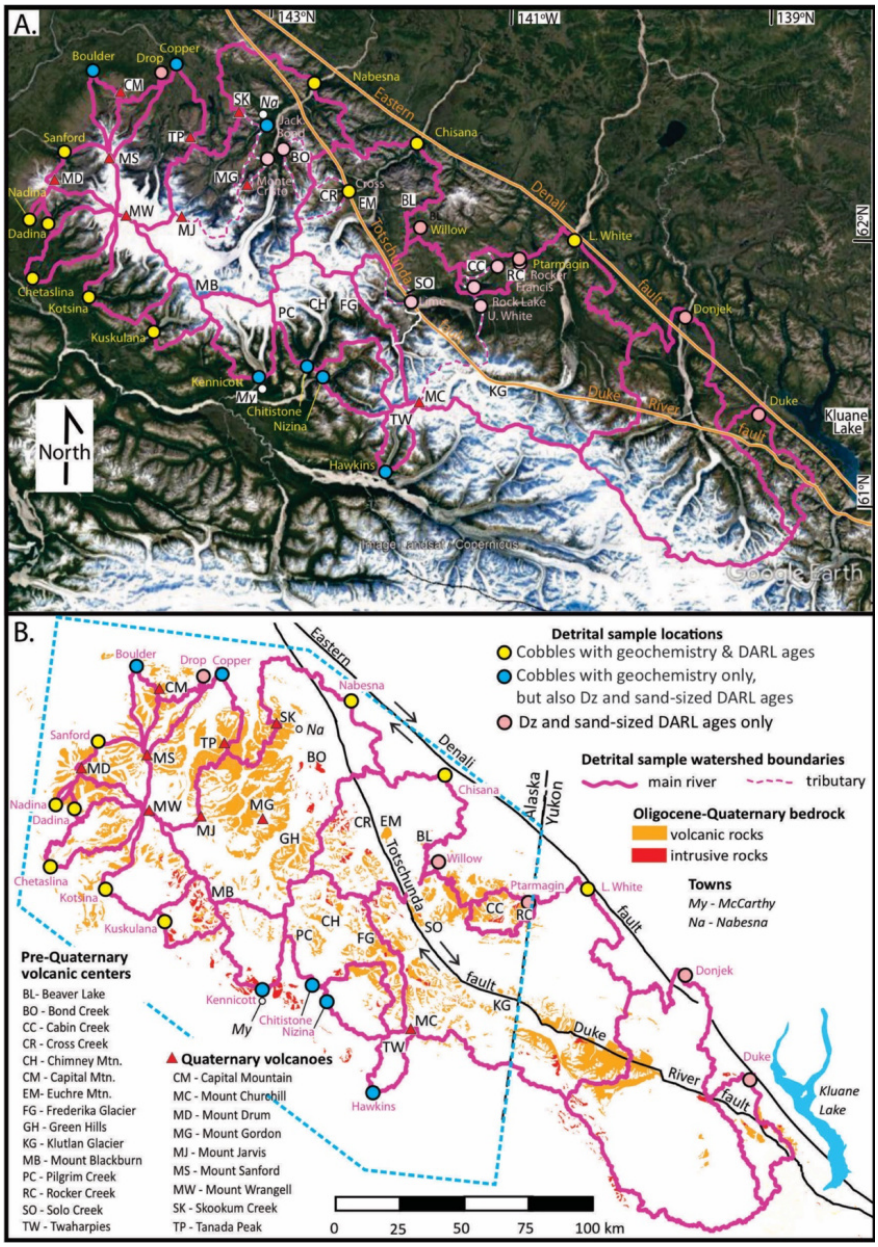

Figure 2: [A] Google Earth (12/19 acquisition date) and [B] geologic map showing watershed boundaries upslope of modern river samples (pink lines), exposed Wrangell Arc volcanics (orange polygons) and intrusions (red polygons), and regional strike-slip faults (black lines). Ice (white in [A]) currently makes up 29 % of the surface area of the sampled watersheds. The dashed blue polygon in [B] is an outline of watershed maps depicted in Figures 6, 10, and 11. Figure after Trop et al. [2022].

by ice fields or glaciers, which effectively restricts access to the rocks beneath this ice [Trop et al. 2022]. However, major river systems drain glaciated watersheds within the Wrangell Arc, thereby providing a sampling mechanism for many of these inaccessible rock units and eroded debris. The sizable spatial extent of the Wrangell Arc, as well as expansive ice cover, large river drainage networks, and the availability of published bedrock (and detrital) ages and bedrock geochemical data, allow for comparisons. Hence, this magmatic arc is an excellent location to implement the use of glacial-fluvial igneous cobbles as an indirect method for petrogenetic-focused, bedrock sampling.

This study focuses on one key question: do the age and composition populations of the igneous cobbles from modern Wrangell Arc rivers reflect the existing bedrock record? We demonstrate that Wrangell Arc igneous cobbles confirm the conclusions of previous geochemical bedrock studies [e.g. Richter et al. 1990; Preece and Hart 2004; Trop et al. 2012; Berkelhammer et al. 2019; Brueseke et al. 2019; Trop et al. 2022] and capture how magma compositions changed, both temporally and spatially, as the Wrangell Arc initiated and grew. Overall, we show that igneous cobbles can be used to indirectly sample bedrock, at the scale of a volcanic arc, and thus can be implemented in other locations where field

conditions limit access to bedrock or as an efficient sampling technique for characterizing watershed-scale bedrock areas.

2 Geologic framework

The Wrangell Arc is a NW–SE trending continental volcanic arc that initiated by ~30 Ma [Brueseke et al. 2019], has experienced continuous magmatism since inception [Trop et al. 2022], and extends from south-central Alaska into the neighboring Yukon Territory of Canada (Figure 1). The Wrangell Arc occurs where the Yakutat microplate subducts beneath the North American plate and undergoes flat or shallow subduction [Bauer et al. 2014]. The Yakutat microplate is interpreted as a wedge-shaped oceanic plateau [Worthington et al. 2012] that originated at lower latitudes at ~50 Ma and was translated ~1900 km northward to its current location along the Fairweather-Queen Charlotte fault system [Plafker and Berg 1994; Wells et al. 2014]. Major strike-slip faults (Denali fault, Totschunda fault, and Duke River fault) also interact with the Wrangell Arc, creating an intersection between convergent and transform margin tectonics [Berkelhammer et al. 2019; Trop et al. 2022, Figure 1]. The Wrangell Arc is part of the greater Wrangell volcanic belt, which extends eastward into Yukon Territory and includes arc and leaky transform magmatism [Skulski et al. 1991; 1992, Figure 1]. Data from the present study focus on only the Wrangell Arc, which includes the active Wrangell volcanic field, although previous results from the eastern Wrangell volcanic belt (Yukon) are used here for interpretations and context. Previous geological investigations in the Wrangell Arc reveal magmatism consists of four distinct geochemical groups that vary in space and time (Figure 3). The four groups are:

1. ubiquitous and voluminous “typical” calc-alkaline arc magmatism [Skulski et al. 1991; 1992; Preece and Hart 2004; Trop et al. 2012; Berkelhammer et al. 2019; Brueseke et al. 2019];

2. low-volume alkaline magmas (alkali basalt, hawaiite, and mugearite) restricted to the eastern Wrangell volcanic belt (Yukon) adjacent to the Denali and Duke River faults, sourced from enriched ocean island basalt-like mantle [Skulski et al. 1991; 1992] (not depicted on Figure 3);

3. spatially restricted voluminous transitional tholeiitic magmatism in the western and central Wrangell Arc associated with intra-arc extension [Preece and Hart 2004; Trop et al. 2012; Berkelhammer et al. 2019; Brueseke et al. 2019];

4. adakitic magmatism previously restricted to two Quaternary volcanoes; Mount Drum and Mt. Churchill [Preece and Hart 2004; Preece et al. 2014] and the ~30–17 Ma Wrangell Arc Sonya Creek volcanic field [Berkelhammer et al. 2019] that formed via melting of the subducting Yakutat slab [Berkelhammer et al. 2019].

Based on a compilation of bedrock and detrital studies, Wrangell Arc magmatism initiated at ~30 Ma in an ~75-km-wide swath along and between the Totschunda fault and the Denali faults [e.g. Brueseke et al. 2019]. Then around ~17 Ma Wrangell Arc magmatism migrated southeastward into the Yukon and was focused along the eastern Duke River fault [Trop et al. 2022, Figure 1]. Subsequently at ~13 Ma Wrangell Arc magmatism migrated westward and was focused along the western Duke River fault and southern Totschunda Fault. After ~6 Ma the Wrangell Arc migrated northwestward with magmatism generally focused away from the Totschunda fault [Richter et al. 1990; Trop et al. 2022] linked to increased Pacific-Yakutat to North America convergence rates [e.g. Engebretson et al. 1985; Richter et al. 1990; Brueseke et al. 2023].

3 Methods and materials

3.1 Field methods

Two hundred and thirty-six igneous cobbles longer than 10 cm were collected from 17 modern river bars that surround and drain the Wrangell Arc (206 discussed in this study), from 2015 to 2016. These rivers are: Jacksina (a subdrainage within the Nabesna watershed), Nabesna, Cross Creek (a sub-drainage within the Chisana River watershed), Chisana, White, Hawkins, Chitistone, Nizina, Root, Kuskalana, Kotsina, Chetaslina, Dadina, Nadina, Sanford, Boulder, and the upper Copper (clockwise from the northwest; Figure 2A, B). Detailed information about the watersheds (e.g. bedrock types, % glacial cover, etc.) can be found in Trop et al. [2022]. Access to these remote field sites was by plane and/or helicopter, so restrictions to the collection procedure included:

1. locating a suitable landing site;
2. transportation limits on total sample weight, and
3. time constraints.

We did not perform grid sampling due to the very short time constraints at each site resulting from helicopter and plane-based access concerns (e.g. fuel, pilot daily hour limitations, cost).

We performed a petrographic survey upon arrival at each collection site to determine the variety of igneous lithologies present at the site (Figure 4) and to collect only the least altered of those lithologies. In some cases, collection sites were strategically chosen downstream of major river confluences to capture tributary input. Ten centimeters was used as an efficient minimum size cut-off, to ensure cobble-sized rocks were collected that were large enough for geochemistry and geochemical material splits. We strived to collect unaltered, “fresh” igneous lithologies and we recognize that some bedrock lithologies may not generate cobble-sized detritus (e.g. less durable tuffs). However, given the overall similarity of the cobble method and bedrock results (discussed in detail below), the sampled cobbles closely emulate the sampled bedrock, thus providing a useful bedrock proxy. Individual cobble samples were split into multiple fragments by hammer and roughly half of those fragments were kept for $^{40}Ar/^{39}Ar$ ground mass and mineral phase geochronology analyses; the remaining fragments of each sample were prepared for x-ray fluorescence (XRF) bulk rock geochemical analyses. Prior to XRF analyses, each sample was assessed and given a hand sample description. The descriptions include general textural descriptions (i.e. porphyritic-volcanic, porphyritic-plutonic,

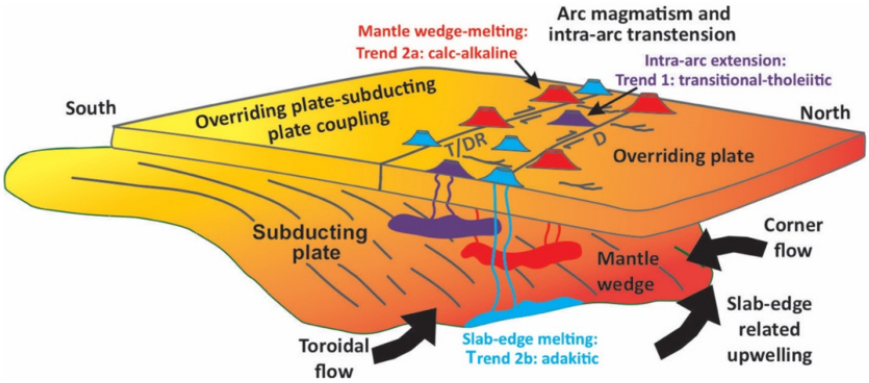

Figure 3: Three-dimensional cartoon of the Wrangell Arc (e.g. the Alaskan portion of the Wrangell volcanic belt) adapted from Berkelhammer et al. [2019]. Depicted are subduction of the Yakutat slab, melt source regions for Wrangell Arc magmas [after Preece and Hart 2004; Brueseke et al. 2019], and major upper-plate strike-slip faults (T/DR—Totschunda/Duke River fault).

Table 1: Age ranges of dated cobbles keyed to river drainage (Figure 2) and possible bedrock sources. *N* = Number of samples.

River	*N*	Possible bedrock sources*	Cobble age range (Ma)
Nabesna	10	Mt. Gordon, Ice Fields Plateau, Skookum Creek, Tp intrusions	28–1
Cross	4	Tp intrusions	27
Chisana	17	Frederika Mountain, Euchre Mountain, Beaver Lake volcanic field	25–6
White	13	Mt. Churchill, Mt. Bona, Castle Mountain, Frederika Mountain, Tp intrusions, Sonya Creek volcanic field	24–9
Kuskulana	16	Mt. Blackburn, Mt. Wrangell	5–3
Kotsina	13	Mt. Wrangell, Mt. Blackburn	2–0.02
Chetaslina	9	Mt. Wrangell	1–0.2
Dadina	11	Mt. Drum, Mt. Wrangell	2–0.3
Nadina	8	Mt. Drum	1–0.2
Sanford	18	Mt. Drum, Mt. Wrangell, Mt. Sanford	2–0.07

* Possible bedrock sources are inferred from Nye [1983]; Preece and Hart [2004]; Richter et al. [2006]; Trop et al. [2012]; Berkelhammer et al. [2019]; Brueseke et al. [2019].

aphanitic, phaneritic, pyroclastic) and are compiled in the supplemental file that contains bulk rock geochemical results.

3.2 Analytical methods

All cobble samples were analyzed previously for $^{40}Ar/^{39}Ar$ ages at the University of Alaska Fairbanks Geochronology laboratory. The majority of samples were analyzed as groundmass single-grain or multi-grain fusion analysis approach and the results have a single-grain and/or multi-grain precision of 1 %. All ages are reported in Supplementary Material 1 Table S1, keyed to sample bulk rock geochemistry. Full $^{40}Ar/^{39}Ar$ details and all of the cobble ages were published in Trop et al. [2022].

Bulk rock geochemical compositions were obtained through XRF analyses of major and trace elements, as well as loss on ignition (LOI). XRF and LOI were completed at Franklin and Marshall College following the method outlined in Mertzman [2000, 2015] and online*. Major elements are reported as wt.% oxide and trace element concentrations are presented as parts per million (ppm). Any analysis with LOI > 3.5 wt.% or wt.% SiO_2 >78 was discarded from the dataset following Trop et al. [2012] and Brueseke et al. [2019]. We also do not report here geochemical data from 17 cobbles that are from pre-Wrangell Arc magmatism [Morter 2017; Trop et al. 2022], thus we report new bulk rock analyses for 206 samples. All major (raw), trace, and rare earth element data are presented in Table S1 (Supplementary Material 1). Fe was split according to Le Maitre [1976] and all major element data used in diagrams and the discussion are reported as anhydrous using the split Fe data.

Preece and Hart [2004], the foundational paper for describing Wrangell Arc volcanic chemical variations, provides a framework for interpreting our new river cobble bulk rock geochemical data. To utilize this framework, we divided our dataset into the three rock suites using the criteria defined by Preece and Hart [2004] (Figure 3 and Figure 8):

1. Trend 1: high TiO_2, transitional-tholeiitic (SiO_2 < 60 wt.% and TiO_2 > 1.15 wt.%; SiO_2 > 60 wt.% and Y > 30 ppm);

2. Trend 2a: low TiO_2, calc-alkaline (SiO_2 > 60 wt.% and TiO_2 < 1.15 wt.%; Y < 30 ppm);

*https://www.fandm.edu/earth-environment/laboratory-facilities/instrument-use-and-instructions

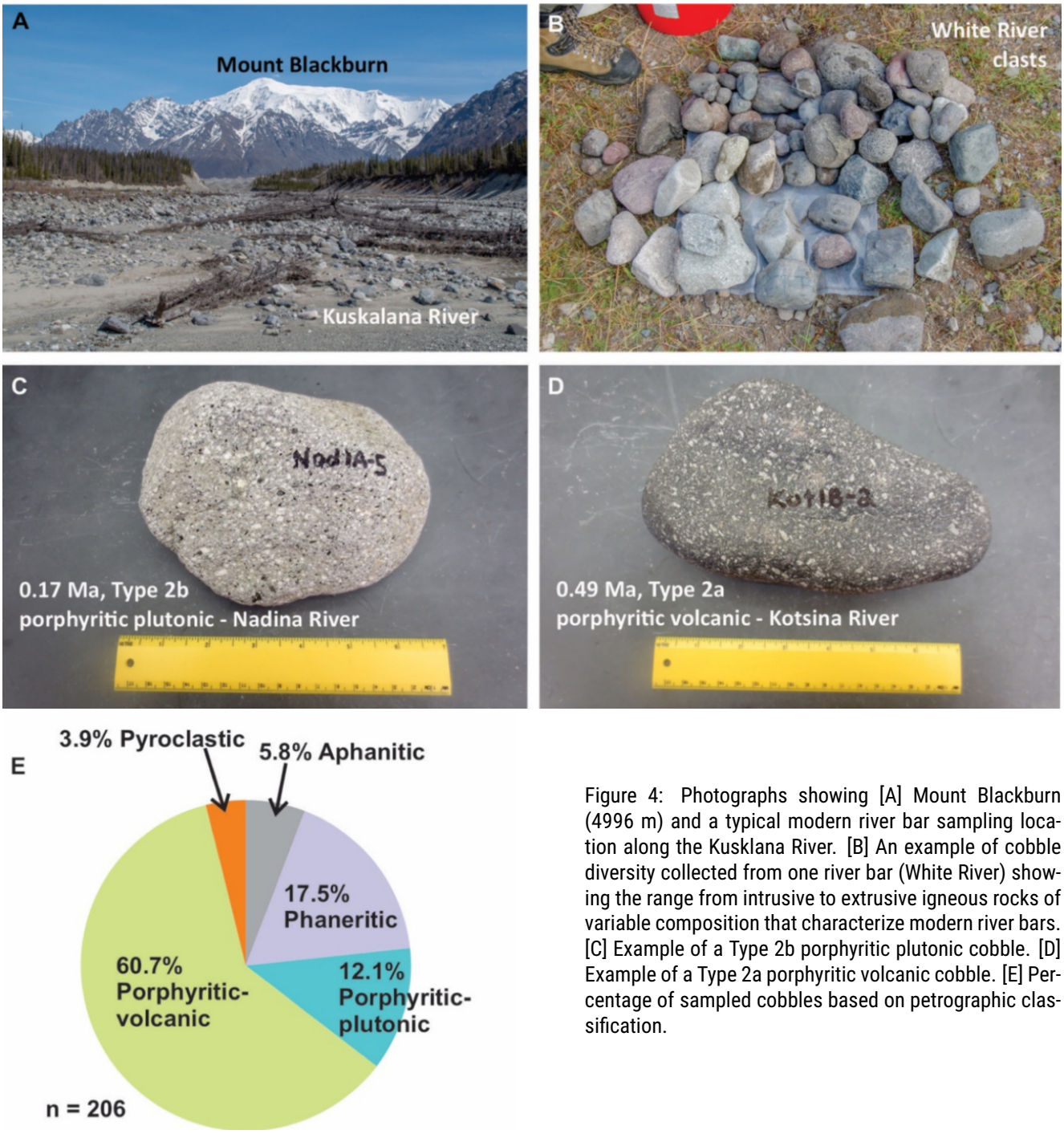

Figure 4: Photographs showing [A] Mount Blackburn (4996 m) and a typical modern river bar sampling location along the Kusklana River. [B] An example of cobble diversity collected from one river bar (White River) showing the range from intrusive to extrusive igneous rocks of variable composition that characterize modern river bars. [C] Example of a Type 2b porphyritic plutonic cobble. [D] Example of a Type 2a porphyritic volcanic cobble. [E] Percentage of sampled cobbles based on petrographic classification.

3. Trend 2b: low TiO_2, calc-alkaline, adakitic (SiO_2 > 60 wt.% and TiO_2 < 1.15 wt.%; Y < 30 ppm, but lower Y than trend 2b).

Trend 1 is associated with intra-arc extension, Trend 2a is formed by flux melting of the mantle wedge (e.g. "normal" subduction), and Trend 2b is also formed by subduction, but has specific trace element (e.g. Sr > ~300 ppm and Y < ~10 ppm) geochemistry that is attributed to partial melting of the subducting slab (i.e. adakitic) [Preece and Hart 2004; Berkelhammer et al. 2019; Brueseke et al. 2019]. Although the geochemical data collected for the present study include most of the necessary parameters to identify rocks considered adakite in the original definition of the word (e.g. subducting slab-melt [Defant and Drummond 1990]) (Sr, Y, La), we lack Yb concentrations and, therefore, refer to our samples as "adakitic", where appropriate.

3.3 Statistical methods

We used the computational program `DZstats` [Saylor and Sundell 2016] to compare cobble geochronology results vs published bedrock, dZ (U-Pb zircon grain ages), and DARL (detrital $^{40}Ar/^{39}Ar$ lithic fragment ages from sand-sized grains) datasets [e.g. Trop et al. 2022]. "Likeness" is a metric that quantifies the degree of overlap between pairs of geochronol-

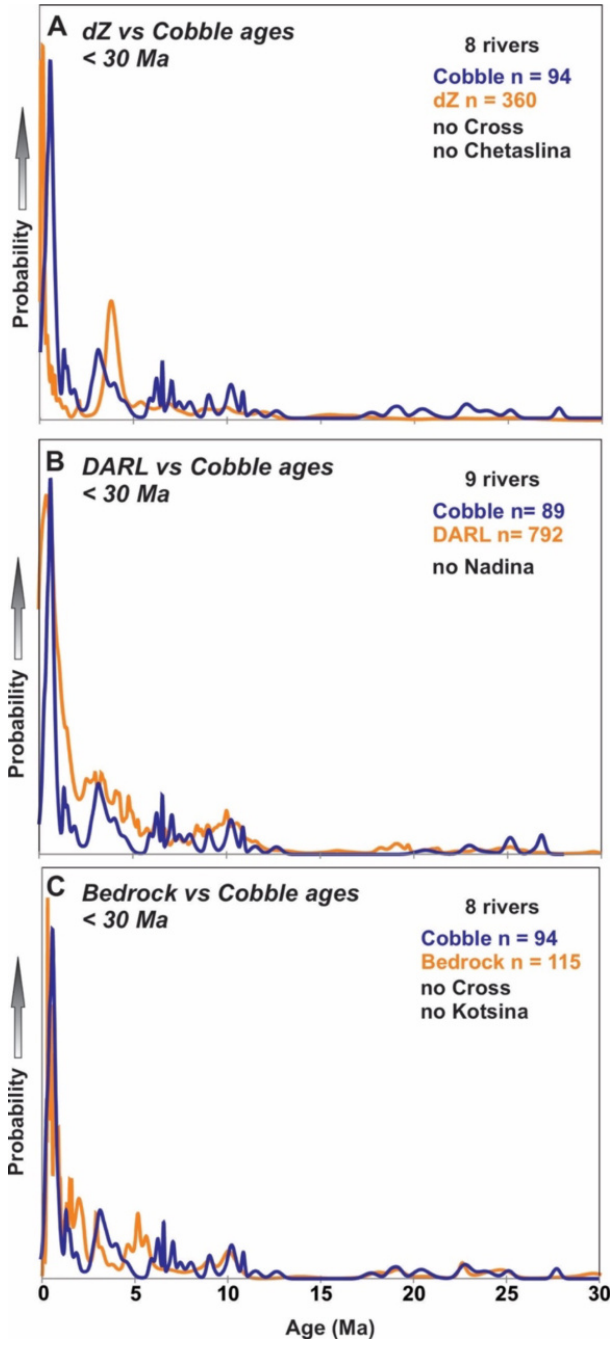

Figure 5: Plots showing overlap in detrital and bedrock ages among the sampled watersheds. [A] Detrital U-Pb zircon ages (dZ) from modern Wrangell Arc rivers compared to cobble $^{40}Ar/^{39}Ar$ ages from the same rivers. [B] Cobble $^{40}Ar/^{39}Ar$ ages compared to $^{40}Ar/^{39}Ar$ ages from sand-sized lithic fragments (DARL) from the same modern Wrangell Arc rivers. [C] Modern river cobble $^{40}Ar/^{39}Ar$ ages compared to published bedrock ages ($^{40}Ar/^{39}Ar$ or K-Ar from minerals, groundmass, or whole rock) from the same river drainages. All data depicted in [A] and [B] from Trop et al. [2022]. Bedrock data from Denton and Armstrong [1969], MacKevett Jr [1976], Nye [1983], Richter et al. [1990], Trop et al. [2012], Brueseke et al. [2019] and Trop et al. [2022]. "No river" = age data from that river is omitted because of the presence of a single data type set or no relevant data.

ogy datasets [Satkoski et al. 2013]. "Similarity" is a metric of the relative abundances of similar ages [Gehrels 2000]. For both likeness and similarity, a value of 1 indicates a perfect match. The Kolmogorov-Smirnov (K-S) test, when applied to geochronology data, can be used to evaluate the likelihood of two geochronology datasets being derived from the same source population [Saylor and Sundell 2016]. The K-S test is based on the K-S statistic (D), which is the maximum difference between the cumulative distribution of the two samples. A K-S p-value <0.05 indicates to the >95 % confidence level that two samples or datasets are not derived from the same population.

4 Results

We report new major and trace element data from 206 individual igneous cobbles, collected from 17 major rivers that drain from the modern Wrangell Arc. We incorporate these geochemical cobble results with $^{40}Ar/^{39}Ar$ data [Trop et al. 2022] from a subset of 100 of the same 206 individual igneous cobbles, with acceptable bulk rock geochemical results from 10 of the rivers (Figure 2B) and summarize the age-chemical relationships below.

4.1 Geochronology

Cobble sample ages range from ~30 Ma to less than 1 Ma (Figure 5). In the dataset we report here, twelve samples range from ~30–17 Ma, from the older portion of the arc (Figure 6). These early arc samples are significant because they reflect the onset of Wrangell Arc magmatism and the origin of the arc, northeast and east of its current location [Brueseke et al. 2019; Trop et al. 2022]. There are no cobble samples from ~17–13 Ma in our entire dataset, which fits geographically with sample locations (e.g. ~17–13 Ma Wrangell field volcanism has only been identified in the Yukon, west of the westernmost White River sample location [Trop et al. 2022]). However, 106 cobble samples remain undated, so the possibility exists, albeit unlikely, that some of these undated cobbles could yield ~17–13 Ma ages. The ~13–1 Ma clast ages demonstrate a shift in magmatic spatial focus to the south, then to the west (Figure 6A). Forty-seven of the dated cobbles are younger than 1 Ma (Figure 5) and come from rivers that drain the western part of the arc, which is the youngest portion [Figure 2 Richter et al. 1990; Preece and Hart 2004; Trop et al. 2022].

We recognize that if our undated cobbles were dated, the relative proportions of cobbles from our age groups might change. We also acknowledge we collected and performed geochemistry analysis on 17 cobbles that are from the older magmatic products in the region that are not included in this work [Morter 2017; Trop et al. 2022]. We cannot know nor address the unknown, hence we focus our main interpretations on the dated cobble dataset. Table 1 summarizes the relevant age data and possible bedrock sources drained by each river where cobbles were collected and dated. Figure 5 shows the cobble ages, compared to other published Wrangell Arc geochronology (bedrock, dZ, and DARL). Figure 6 shows the cobble ages in the spatial context of Wrangell Arc watersheds, compared to published Wrangell Arc bedrock samples from the same drainages.

4.2 Petrographic classification

Hand sample descriptions from all cobbles (dated and undated) are divided into five distinct textural groups: aphanitic, phaneritic, porphyritic-volcanic, porphyritic-plutonic, and pyroclastic; the dominant type is porphyritic-volcanic (60.7 %; Figure 4). Extrusive and intrusive cobbles occur across the sampled watersheds, but pyroclastic cobbles, indicative of explosive eruptions, are reported from only spatially limited locations in Wrangell Arc drainages (Sanford, Chetaslina, Nizina, and Chisana Rivers). Pyroclastic cobbles are also only associated with three age groups: 8–6 Ma, 3–1 Ma, and <1 Ma.

4.3 Bulk rock geochemistry

Geochemical data here are presented in spatial and temporal contexts to illuminate the petrogenetic history of the Wrangell Arc. Each dated cobble sample has been assigned to one of the following age groups: 30–17 Ma 17–13 Ma, 13–8 Ma, 8–6 Ma, 6–3 Ma, 3–1 Ma, and <1 Ma after the compiled temporal-spatial trends established by Trop et al. [2022]. Additionally, over half of the samples analyzed for geochemistry lack age dates; these samples are included in these plots and are coded as "No age."

Our new data overlap the compositions of Wrangell Arc bedrock samples previously reported by Preece and Hart [2004], Trop et al. [2012] (Figures 7, 8, 9), Brueseke et al. [2019], and Berkelhammer et al. [2019]. On the total alkalis versus silica (TAS) diagram of Le Bas et al. [1986], dated Wrangell Arc eruptive products plot as subalkaline to transitional and range from basaltic (trachy) andesite to rhyolite (Figure 7A). Eighty-eight percent of the samples are andesite or dacite and 84 % of the andesites are medium-K. These rocks are primarily <1 Ma, and come from rivers that drain the westernmost part of the Wrangell Arc (e.g. adjacent to active and/or recently dormant volcanoes like Mt. Drum, Sanford, and Wrangell). In an AFM diagram, nearly all Wrangell Arc igneous cobbles follow a calc-alkaline array that overlaps with bedrock sample datasets (Figure 7B).

The igneous cobble dataset reported herein includes samples that largely overlap with the Preece and Hart [2004] classification scheme, as described above in the Methods and materials (Figures 7, 8, 9). Trend 1 and Trend 2a are generally contained in the andesite-dacite-rhyolite (ADR) field on a Sr/Y vs. Y plot whereas Trend 2b falls into the "adakitic" field (Figure 9). Adakitic magmas (Type 2b) generally cluster into two groups, one with ages between ~30–17 Ma and another group with ages <6 Ma (Figure 9). However, cobbles with adakitic signatures span the full history of Wrangell Arc magmatism (Figures 3 and 10). Type 1 transitional-tholeiitic magmatism occurs predominately ~13–6 Ma in the western and central Wrangell Arc (Figure 8) and is associated with intra-arc extension. However, cobbles with intra-arc extension signatures are present with ages also at <1 and 6–3 Ma (Figure 8). Cobbles with "typical" calc-alkaline subduction signatures indicative of melting of subduction-affected mantle wedge (i.e. Trend 2a,) also span the full history of Wrangell Arc magmatism (Figures 7 and 9).

5 Discussion

5.1 Did the cobble geochronology-geochemistry approach replicate bedrock and detrital single grain results?

Statistically, we compared individual river datasets that have corresponding data from the same rivers, hence each comparison involves slightly different drainage combinations and cobble counts. Cobble ages vs. bedrock ages, cobble ages vs. dZ ages, and cobble ages vs. DARL ages all indicate a high degree of likeness and similarity (Table 2, Figure 5). The K-S test indicates the cobble versus bedrock ages and cobble versus DARL ages were derived from the same population. With p-values dropping below 0.05, the K-S test of cobble versus dZ ages indicates these two geochronology datasets may have been derived from different datasets.

Since zircon stability is correlated with felsic over mafic magmatic products this result likely reflects the dZ results being biased by lithology and the dominance of zircon-poor, intermediate composition magmatic products (vs. zircon-bearing felsic rocks) in the Wrangell Arc (Figure 7A). This "failure" is apparently due in part to the Kuskalana River—where the dZ sourced a lot of 3–6 Ma zircons (likely derived from felsic Wrangell Arc rocks) and high N zircon flooded the dataset. The Kuskalana (Figure 2) drains part of the Wrangell Arc that is characterized by felsic intrusives that are interpreted to be syn-volcanic (e.g. granitoids mapped as unit Tp [Richter et al. 1995; 2006]) to the ~3.4–5 Ma Mt. Blackburn volcano. The data we present from this river is an excellent example of fertility and compositional concerns when using just one type of detrital dataset to interpret the geochronological and/or geochemical characteristics of modern drainages. Thus, solely utilizing the detrital zircon record to evaluate the entirety of volcanism at a given volcano, volcanic field, or volcanic arc, should be discouraged; dZ data generally is most reflective of the felsic history of magmatism [Dickinson 2008]. Overall, the cobble geochronology approach mimicked the age results from the bedrock, dZ, and DARL datasets (Figure 12, Table 2).

The results from this study show that the sampled cobbles largely reproduce the known bedrock record in geochemical, temporal, and spatial contexts (Figures 6, 10–12) and the known bedrock record does not contain any geochemical types that are not present in the cobble record (Figure 7). Notably, the percentage of geochemical types (e.g. Trends 1, 2a, 2b) of bedrock and cobbles for each age bin shown on Figure 12, are very similar. The geochemical compositions of cobbles closely match the geochemistry of the bedrock exposed upslope; Trend 2 cobbles are spatially and temporally present in rivers that drain the extent of the Wrangell Arc, whereas Trend 1 cobbles are not found in southwestern Wrangell Arc rivers (Figure 10 and Figure 11).

The ages represented in the cobble record span the lifetime of the arc (~30 Ma to present) as known from bedrock and detrital age datasets [Trop et al. 2022]. Unlike the detrital ages from volcanic-lithic sand and zircons presented in Trop et al. [2022], we can link magmatic events of different magma types (i.e. Trend 1, Trend 2a, Trend 2b) to specific time intervals throughout the history of the Wrangell Arc because

Table 2: Statistical comparisons of Wrangell Arc cobble ages (cobble rivers = rivers where we sampled cobbles) and other Wrangell Arc age datasets from the same drainages (e.g. dated bedrock, dZ U-Pb ages, and $^{40}Ar/^{39}Ar$ lithic ages [e.g. DARL—sand-sized lithic fragments]). Calculations were performed using `DZstats` [Saylor and Sundell 2016]. Blue shaded cells denote comparisons between data from the same river subsets. Orange-colored text denotes failed KS test value for cobble ages vs. dZ ages from the same rivers, indicating the cobbles and the dZ are not derived from the same population (P <0.05, so failure).

Likeness value	Cobble rivers with		
	bedrock ages	dZ ages	DARL ages
Bedrock ages from cobble rivers	0.7195	0.7222	0.6944
dZ ages from cobble rivers	0.6983	0.6807	0.6759
DARL ages from cobble rivers	0.7821	0.7925	0.7840

Similarity value	Cobble rivers with		
	bedrock ages	dZ ages	DARL ages
Bedrock ages from cobble rivers	0.7050	0.7012	0.6943
dZ ages from cobble rivers	0.6376	0.6361	0.6335
DARL ages from cobble rivers	0.6516	0.6575	0.6521

K-S test p value	Cobble rivers with		
	bedrock ages	dZ ages	DARL ages
Bedrock ages from cobble rivers	0.4619	0.4817	0.2699
dZ ages from cobble rivers	0.0013	0.0009	0.0003
DARL ages from cobble rivers	0.0499	0.0259	0.0590

K-S test D statistic	Cobble rivers with		
	bedrock ages	dZ ages	DARL ages
Bedrock ages from cobble rivers	0.1173	0.1152	0.1385
dZ ages from cobble rivers	0.2213	0.2259	0.2456
DARL ages from cobble rivers	0.1482	0.1600	0.1462

of our combined cobble geochemistry-geochronology. Consequently, this cobble technique, together with detrital ages from sand-sized volcanic-lithics and zircons, has allowed for a better understanding of the age and migration patterns of the Wrangell Arc. When considered with the detrital sand and bedrock age data, the cobble data fit in well with the overall history of the Wrangell Arc and reproduce the ~17–13 Ma gap in magmatism seen in the western and central Wrangell Arc bedrock and detrital records [Trop et al. 2022] (Figures 6, 11, and 12).

Within our dataset, cobble dates are more heavily distributed toward younger ages than the published bedrock data. Nearly half of the cobble ages are <1 Ma and cobble samples become sparser further back in time. The 30–17 Ma age category only has 12 cobbles but covers the largest and oldest age range in our classification scheme. This is most likely due to not sampling cobbles from the Sonya Creek Volcanic Field, the oldest part of the Wrangell Arc [Berkelhammer et al. 2019]. It is also probable that older Wrangell Arc bedrock is covered by younger volcanic products, limiting exposure for cobble sourcing. Nevertheless, older samples (~30–17 Ma) are still present in the cobble record in drainages that we sampled and provide meaningful and significant data and provide critical data relating to the cobble and bedrock records.

5.2 Wrangell Arc tectonic reconstruction buttressed through cobble geochemistry

5.2.1 *Melting of the subduction-affected mantle wedge (Trend 2a)*

Trend 2a (calc-alkaline) cobbles are distributed across the spatial extent of the arc (Figures 3, 10, and 11). Trend 2a signatures are also temporally and spatially pervasive throughout the bedrock record [Preece and Hart 2004; Brueseke et al. 2019]. The tectonic implication of these cobble and bedrock Trend 2a occurrences through time is that subduction processes have been continuous throughout the ~30 Ma history of the Wrangell Arc.

5.2.2 *Slab-edge melting (Trend 2b)*

Numerous petrologic mechanisms have been proposed to produce magmas that are described as “adakite” [Zhang et al. 2019], and we acknowledge that the term is not always appropriately applied to reflect magma derivation via slab-melting. However, in the Wrangell Arc, prior geochemical studies have

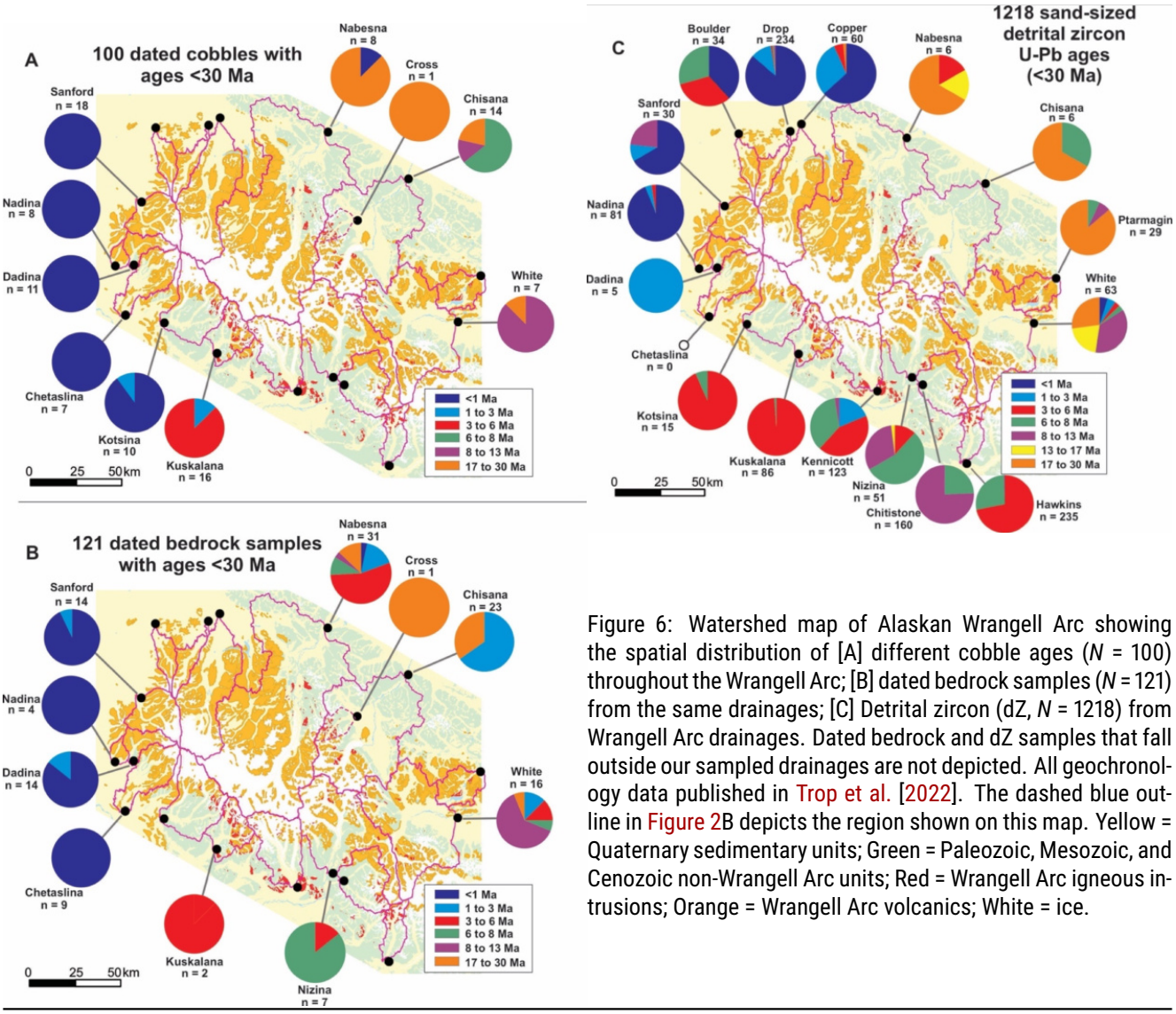

Figure 6: Watershed map of Alaskan Wrangell Arc showing the spatial distribution of [A] different cobble ages (N = 100) throughout the Wrangell Arc; [B] dated bedrock samples (N = 121) from the same drainages; [C] Detrital zircon (dZ, N = 1218) from Wrangell Arc drainages. Dated bedrock and dZ samples that fall outside our sampled drainages are not depicted. All geochronology data published in Trop et al. [2022]. The dashed blue outline in Figure 2B depicts the region shown on this map. Yellow = Quaternary sedimentary units; Green = Paleozoic, Mesozoic, and Cenozoic non-Wrangell Arc units; Red = Wrangell Arc igneous intrusions; Orange = Wrangell Arc volcanics; White = ice.

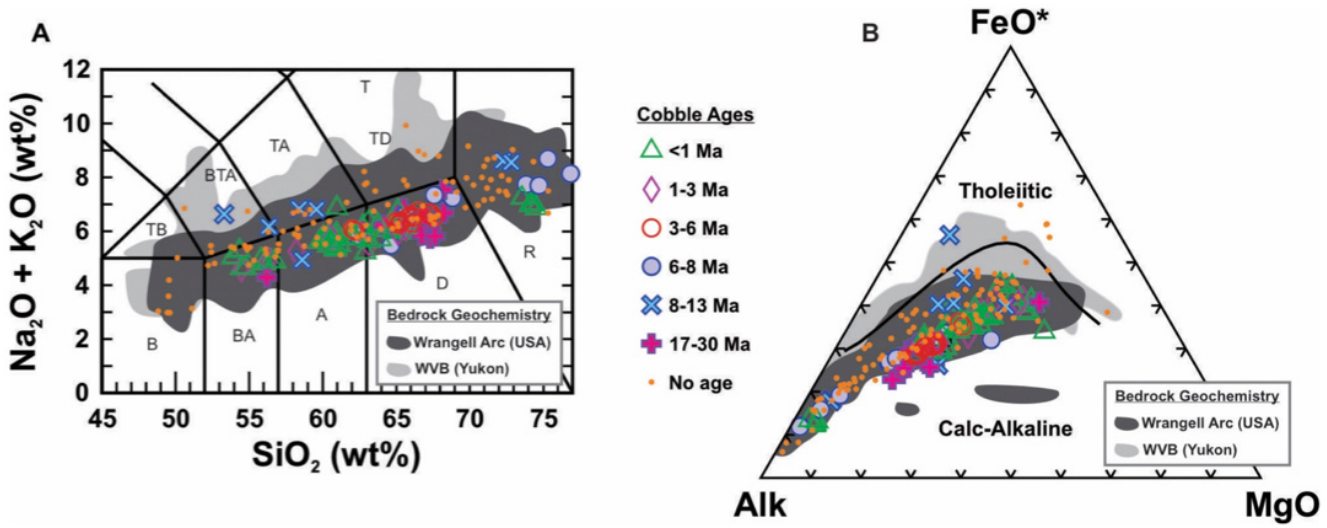

Figure 7: [A] Total alkalies versus silica diagram from cobble samples ([Le Bas et al. 1986], coded by age, compared to bedrock record [from Preece and Hart 2004; Trop et al. 2012], Wrangell volcanic belt (WVB [Yukon]) data from Skulski et al. [1991, 1992]. [B] AFM diagram after Irvine and Baragar [1971]. All other figures that depict geochemical data use the symbols and fields depicted in this legend.

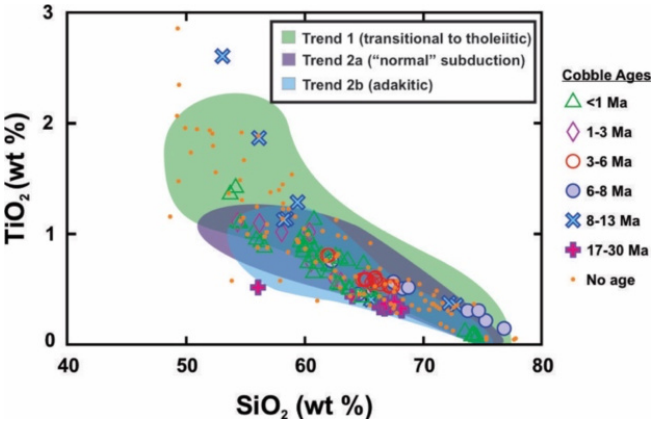

Figure 8: TiO_2 vs. SiO_2 , comparing geochemistry of cobbles and Wrangell Arc bedrock, where symbols are cobble data classified according to Preece and Hart [2004] illustrating the larger range of TiO_2 values at SiO_2 < 60 wt.% than at SiO_2 > 60 wt.% that characterize Trend 1 magmas.

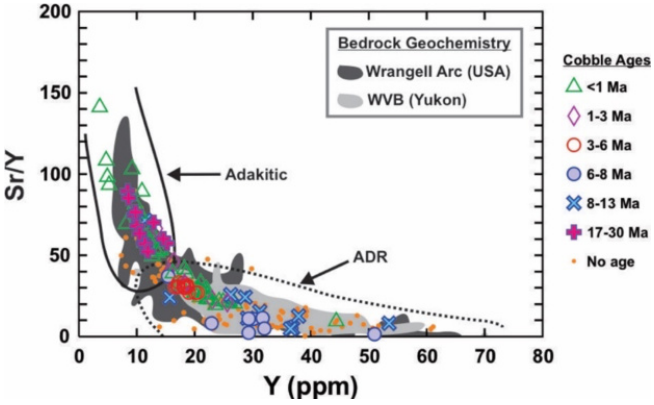

Figure 9: Comparison of the geochemistry of cobbles to Wrangell Arc bedrock and adakite vs. non-adakitic andesite-dacite-rhyolite (ADR) fields for arc rocks after Defant and Drummond [1990].

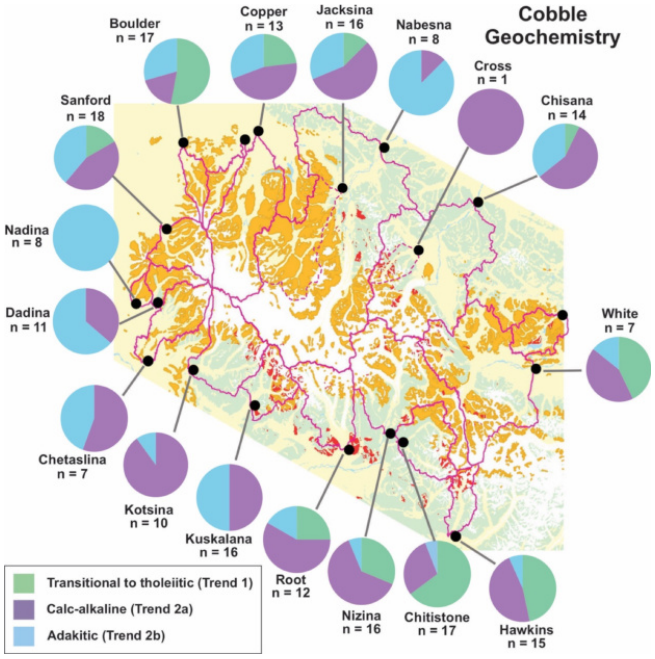

Figure 10: Summary of cobble geochemical data (n = 206) showing the distribution of magma types in each sampled watershed across the Wrangell Arc classified into Trends 1, 2a, and 2b as outlined in Preece and Hart [2004] and this paper. Figure includes undated and dated cobbles.

documented adakitic magmatism consistent with the melting of eclogitized, subducting oceanic crust (e.g. Trend 2b of Preece and Hart [2004] and Berkelhammer et al. [2019]) and regional geophysical studies document mantle upwelling adjacent to an imaged slab edge/tear bordering the young, western-most WVF (e.g. slab tear formation ca. ~1 Ma [Mann et al. 2022; Brueseke et al. 2023]). Thus, it is likely that adakitic Wrangell Arc magmas reflect slab-edge and/or slab melting [Brueseke et al. 2019].

Throughout the ~30 Ma history of the Wrangell Arc, Trend 2b (e.g. adakitic) cobbles are distributed across the arc (Figure 10 and Figure 11). There are Trend 2b cobbles from every river we sampled (except for Cross Creek, a tributary to the larger Chisana drainage). However, cobbles with Trend 2b signatures are more abundant during the oldest (~30–17 Ma) and youngest (<6 Ma) Wrangell Arc magmatism, i.e., during arc initiation and recent magmatism, respectively (Figure 10 and Figure 11). Eleven of the twelve oldest (~30–17 Ma) cobbles in the dataset are Trend 2b, with only one cobble classified as Trend 2a (Figure 11 and Figure 12).

Trend 2b magmas are recognized in the bedrock at Mt. Drum and Mt. Churchill [Preece and Hart 2004]. Mt Drum and Mt. Churchill are the northwestern- and southeastern-most volcanoes in the active Wrangell Arc, respectively (Figure 2), and are coincident with the inferred tear in the Yakutat slab and the slab edge [Mann et al. 2022; Brueseke et al. 2023]. Trend 2b magmas are also recognized in the oldest ~30–17 Ma bedrock of the Wrangell Arc [Berkelhammer et al. 2019; Brueseke et al. 2019] which had a ~170 km arc length generally trending east-west [Trop et al. 2022]. During this early arc period (~30–17 Ma), after Yakutat slab subduction had initiated, subducting slabs and slab edges would be expected to be more prone to melting due to increased thermal gradients [Sajona et al. 1993], which may explain the widespread distribution of these Trend 2b occurrences in the bedrock and cobble record during Wrangell Arc initiation. Overall, these cobble and bedrock Trend 2b spatial occurrences indicate a component of slab melting across the entire arc and that persistent slab edge melting may be a geochemical signature of slab edge environs. However, more work is needed to determine the petrogenetic environ responsible for adakitic magmatism during the "mature" stage of the Wrangell arc (e.g. ~13–2 Ma), prior to the development of the Yakutat slab tear (~1 Ma).

5.2.3 *Intra-arc extension (Trend 1)*

The most spatially restricted magma type in the cobble record is Trend 1 (transitional-tholeiitic), which is consistently absent

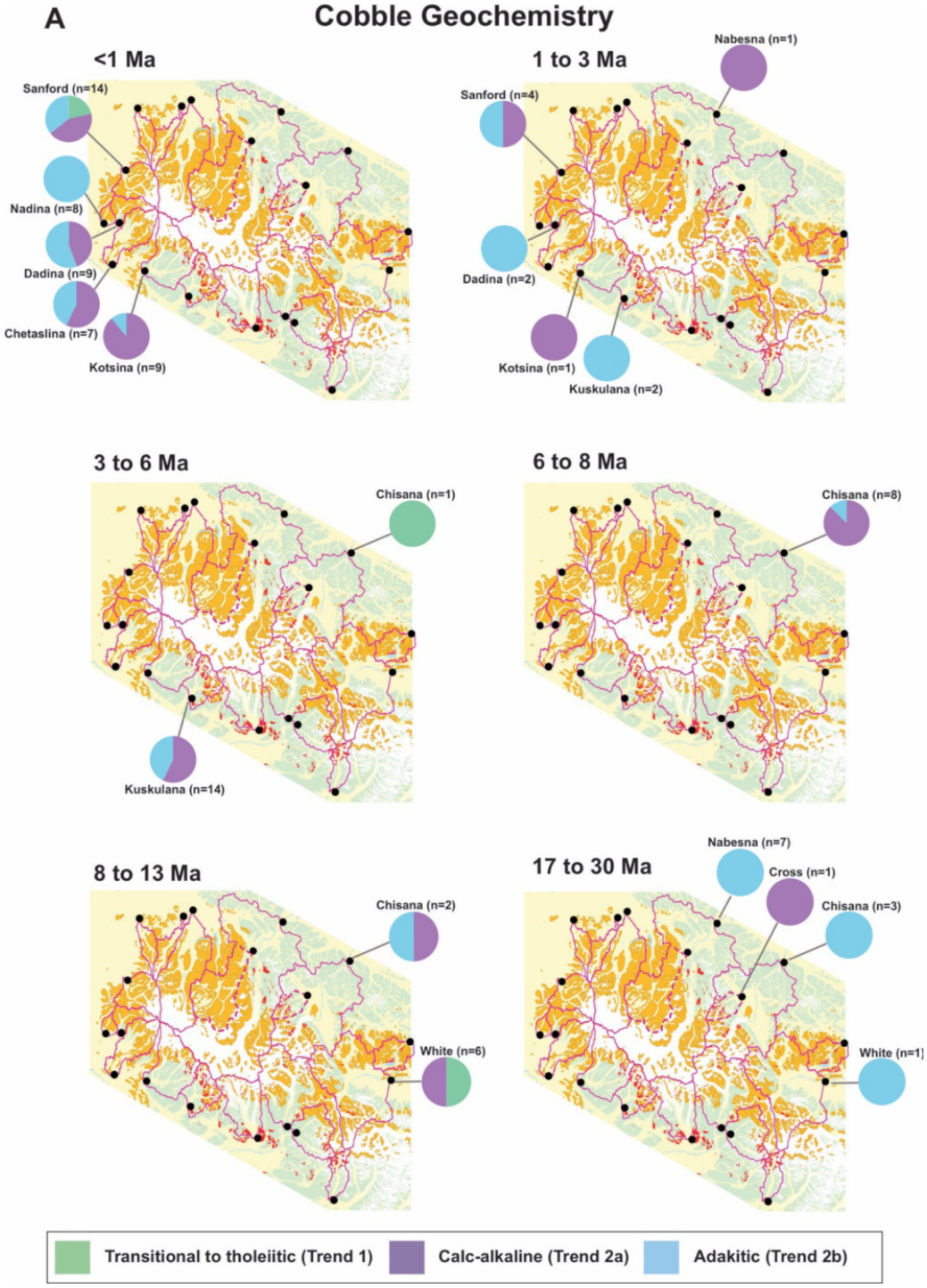

Figure 11: [A] Watershed maps depicting dated cobble geochemistry (*N* = 100) through time.

from the Nadina River southeastward to the Kuskulana River (Figure 10 and 11). Dated Trend 1 cobbles are temporally restricted to <1 Ma and 3–6 Ma in the northern Wrangell Arc from the Chisana and Sanford Rivers, and ~13–8 Ma in the central Wrangell Arc sourced from the White River (Figure 11). The Hawkins, Chitistone, and Nizina cobble dataset lack age data, but have a large percentage of Trend 1 cobbles (65, 50, and 31 % respectively). These drainages have ~13–3 Ma dZ data adding support to this being a time period of intra-arc extension, as documented by Trop et al. [2012]. Bedrock studies [Preece and Hart 2004; Trop et al. 2012; Keast et al. 2016; Berkelhammer et al. 2019] only show localized occurrences of Trend 1 magmas, which stand in contrast to expansive spatial occurrences of Trends 2a and 2b. Furthermore, there is no relationship between times of increased activity on the Totschunda fault (~6 Ma to Present [Waldien et al. 2018]) and/or decreased activity along the eastern Denali fault [Waldien et al. 2021] with documented times of intra-arc extension in the Wrangell Arc (Figure 1). Slip along these

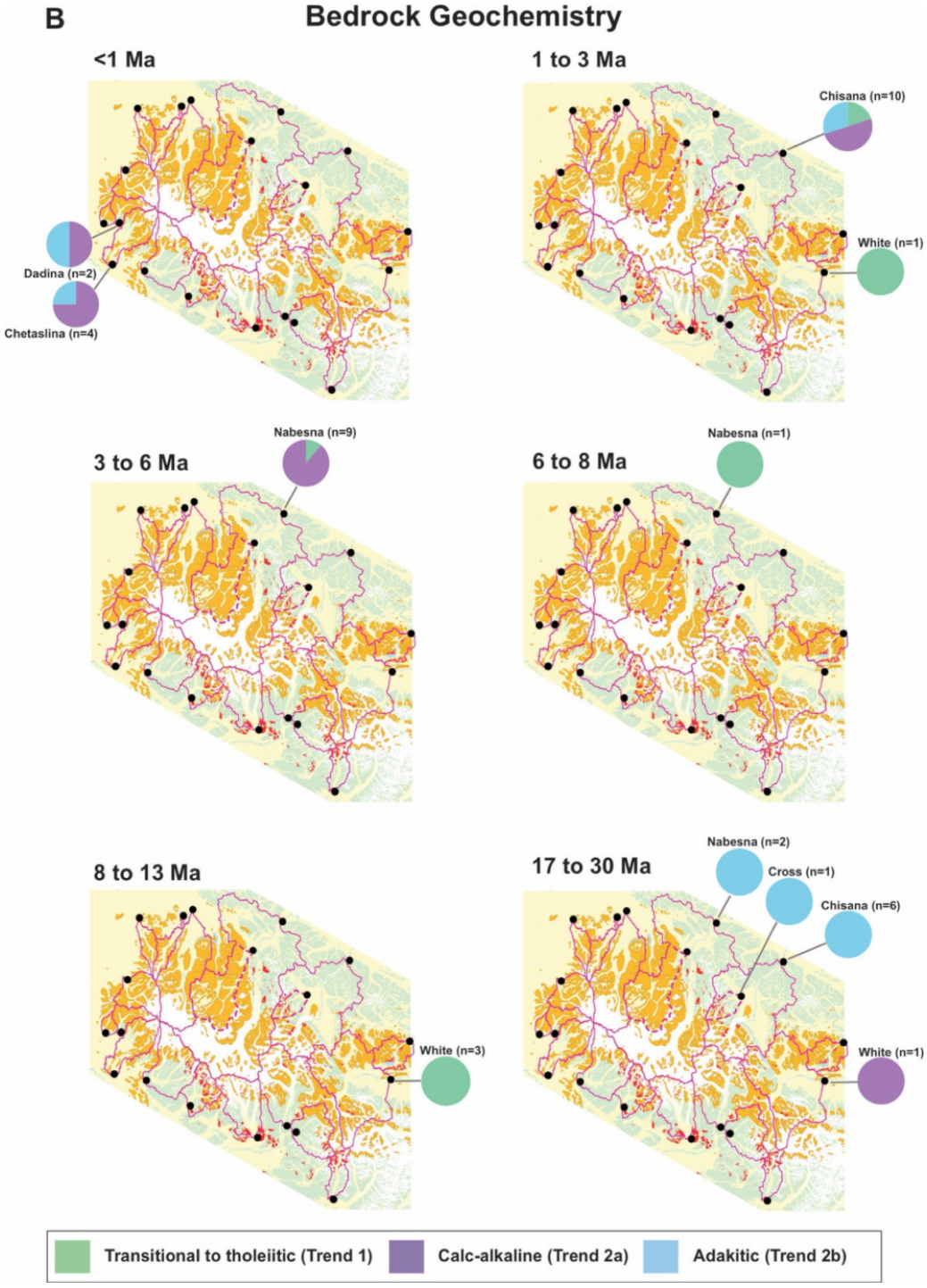

Figure 11: [B] Watershed maps depicting dated bedrock geochemistry (N = 40) through time.

major faults is concurrent and likely Wrangell Arc intra-arc extension is a response to this transtensional environment.

The ability of the cobble data to broadly reproduce the geochemistry and geochronology resulting from detailed bedrock-based field mapping and sampling is encouraging because this suggests the methodology applied here can be successfully applied in other localities, regardless of glacial, tectonic, or volcanic setting. This approach may need to be modified in other settings to account for the number of regional drainages and overall aridity. However, even in a desert environment, like parts of the eastern side of the Andes arc, we suggest our method could be applied. For example, recent debris flow deposits and other volcaniclastic sediments (e.g. lahars) will still contain cobbles and sediment derived from bedrock in their respective drainages. The cobble approach is an efficient and cost-effective way of indirectly sampling bedrock in locations where field conditions limit sampling capabilities. This approach can also help scientists who have mobility-related disabilities participate in field sampling campaigns of geologic settings that might otherwise be inaccessible [Chiarella and

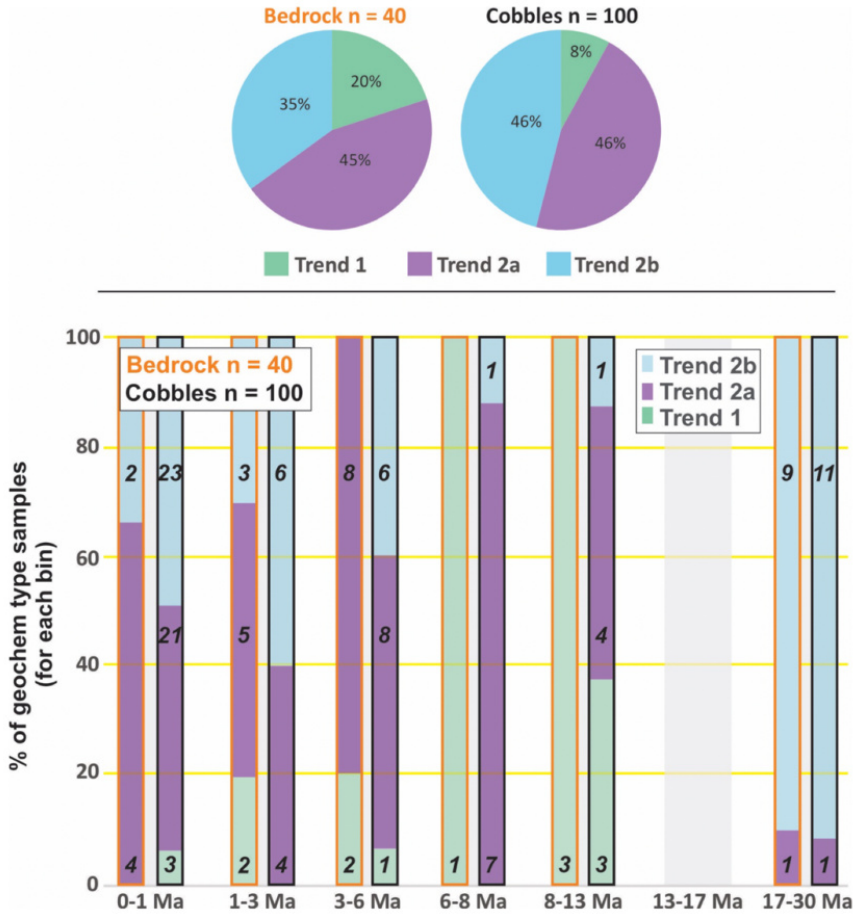

Figure 12: Summary of magma types (e.g. Trends 1, 2a, 2b) for cobble data and bedrock data (with bulk rock geochemistry) from sampled Wrangell Arc rivers (Figure 6). Samples in the histograms include the full datasets for the sampled rivers and are normalized for each time period, to fully depict how the cobble geochemical-age distributions emulate the bedrock-geochemical age record across the volcanic arc. The numbers in the bar segments are the number of individual samples in each category. Bedrock data is always the left bar for each time period, highlighted by orange outlines; cobble data is always the right bar for each time period, highlighted by black outlines.

Vurro 2020]. The geochemical-geochronological cobble application has the potential to provide access to lithologies that are otherwise inaccessible due to ice cover or other hindrances that restrict bedrock sampling. This type of sample collection method can also be easily added on to a more ambitious field study with relative ease to complement any bedrock record and increase the robustness of an entire dataset, and we suggest the tandem cobble method will work in volcanic arc-settings, or other igneous-hosted terrains, that are dissected by fluvial systems. The tandem cobble methods can also be applied to the sampling of cobbles from ancient and modern glacial moraines [Enkelmann and Ehlers 2015] as long as samples are collected randomly along an individual moraine to avoid sourcing biases due to glacier advective transport dynamics [Bernard et al. 2020].

6 Conclusions

Bulk rock geochemistry and geochronology of cobbles from modern rivers draining the Wrangell Arc closely match previously reported bedrock datasets that document subduction, slab-edge melting, and intra-arc extension during the past ~30 Ma in the Wrangell Arc due to subducting slab processes (i.e. slab rollback and change in subduction direction) and upper-plate strike-slip processes (i.e. transtensional and dextral movement along the Totschunda, Denali, and Duke River faults).

The Wrangell Arc was continuously active from 30 Ma to the present as indicated by the ubiquitous occurrence of cobbles and bedrock with calcalkaline signatures through space and time. Slab-melting, as inferred from adakitic samples, was prominent early in the arc history, again late ca. ~1 Ma (e.g. coeval with the formation of the Yakutat slab tear just west of the arc), with sparse occurrences in intervening years. Intra-arc extension as indicated by cobbles with tholeiitic compositions, are temporally limited to <1 Ma, 6–3 Ma, and 13–8 Ma and only found in eastern drainages.

This tandem geochemical-geochronological cobble approach provides a time- and cost-effective method to obtain geochemical and geochronological constraints on regions where bedrock sampling is limited by exposure and/or access. We show here that the tandem detrital approach works at the scale of a 200-km-long continental arc and suggest that this technique can be applied in other settings where access to bedrock sampling may be difficult but access to river detritus is relatively easy. The combined geochemical-geochronological cobble approach can also be applied in other settings dominated by igneous bedrock that is dissected by active fluvial systems.

Author Contributions

This research was part of Morter's M.S. thesis at Kansas State. Brueseke, Trop, Benowitz, Davis, and Morter collected the samples, Mertzman did the bulk rock XRF analyses on samples prepared by Morter, and Kirby mapped the geologic characteristics and areal extent of the sampled watersheds. Brueseke, Benowitz, Trop, and Morter wrote the manuscript and made the figures.

Acknowledgements

This study was made possible in part by funding from NSF to Brueseke (EAR-1450689), Benowitz and P. Layer (EAR-1450730), and Trop (EAR-1450687). We thank everyone at Devil's Mountain Lodge for field/air support; Last Frontier Air Ventures, Soloy Helicopters, Wrangell Mountain Air; NPS personnel at Wrangell-St. Elias National Park and Preserve for access to field sites; Arizona LaserChron Center for assistance in collecting U-Pb geochronologic data, and Sam Berkelhammer for assistance in the field. We thank Anita Grunder and one anonymous reviewer for their constructive feedback, and to Editor Lynne Elkins for handling our manuscript.

Data Availability

All supporting analytical data can be found online as Supplementary Material and also are available at the following link: https://doi.org/10.5281/zenodo.7916454 (embargoed until Sept. 1, 2023).

References

Amidon, W. H., D. W. Burbank, and G. E. Gehrels (2005). "Construction of detrital mineral populations: insights from mixing of U-Pb zircon ages in Himalayan rivers". *Basin Research* 17(4), pages 463–485. ISSN: 1365-2117. DOI: 10.1111/j.1365-2117.2005.00279.x.

Barth, A., J. Wooden, C. Jacobson, and R. Economos (2013). "Detrital zircon as a proxy for tracking the magmatic arc system: The California arc example". *Geology* 41(2), pages 223–226. DOI: 10.1130/g33619.1.

Bauer, M. A., G. L. Pavlis, and M. Landes (2014). "Subduction geometry of the Yakutat terrane, southeastern Alaska". *Geosphere* 10(6), pages 1161–1176. DOI: 10.1130/ges00852.1.

Benowitz, J. A., K. Davis, and S. Roeske (2019). "A river runs through it both ways across time: 40Ar/39Ar detrital and bedrock muscovite geochronology constraints on the Neogene paleodrainage history of the Nenana River system, Alaska Range". *Geosphere* 15(3), pages 682–701. DOI: 10.1130/ges01673.1.

Berkelhammer, S. E., M. E. Brueseke, J. A. Benowitz, J. M. Trop, K. Davis, P. W. Layer, and M. Weber (2019). "Geochemical and geochronological records of tectonic changes along a flat-slab arc-transform junction: Circa 30 Ma to ca. 19 Ma Sonya Creek volcanic field, Wrangell Arc, Alaska". *Geosphere* 15(5), pages 1508–1538. ISSN: 1553-040X. DOI: 10.1130/ges02114.1.

Bernard, M., P. Steer, K. Gallagher, and D. L. Egholm (2020). "Modelling the effects of ice transport and sediment sources on the form of detrital thermochronological age probability distributions from glacial settings". *Earth Surface Dynamics* 8(4), pages 931–953. DOI: 10.5194/esurf-8-931-2020.

Brueseke, M. E., J. A. Benowitz, A. T. Bearden, M. E. Mann, and D. P. Miggins (2023). "Subduction disruption, slab tears: ca. 1Ma true collision of an 30-km-thick oceanic plateau segment recorded by Yakutat slab nascent tear magmatism". *Terra Nova* 35(1), pages 49–57. ISSN: 1365-3121. DOI: 10.1111/ter.12628.

Brueseke, M. E., J. A. Benowitz, J. M. Trop, K. N. Davis, S. E. Berkelhammer, P. W. Layer, and B. K. Morter (2019). "The Alaska Wrangell Arc: 30 Ma of subduction-related magmatism along a still active arc-transform junction". *Terra Nova* 31(1), pages 59–66. ISSN: 1365-3121. DOI: 10.1111/ter.12369.

Capaldi, T. N., B. K. Horton, N. R. McKenzie, D. F. Stockli, and M. L. Odlum (2017). "Sediment provenance in contractional orogens: The detrital zircon record from modern rivers in the Andean fold-thrust belt and foreland basin of western Argentina". *Earth and Planetary Science Letters* 479, pages 83–97. ISSN: 0012-821X. DOI: 10.1016/j.epsl.2017.09.001.

Carley, T., C. Miller, O. Sigmarsson, M. Coble, C. Fisher, J. Hanchar, A. Schmitt, and R. Economos (2017). "Detrital zircon resolve longevity and evolution of silicic magmatism in extinct volcanic centers: A case study from the East Fjords of Iceland". *Geosphere* 13(5), pages 1640–1663. ISSN: 1553-040X. DOI: 10.1130/ges01467.1.

Chiarella, D. and G. Vurro (2020). "Fieldwork and disability: an overview for an inclusive experience". *Geological Magazine* 157(11), pages 1933–1938. ISSN: 1469-5081. DOI: 10.1017/s0016756820000928.

Clift, P. D., H. V. Long, R. Hinton, R. M. Ellam, R. Hannigan, M. T. Tan, J. Blusztajn, and N. A. Duc (2008). "Evolving east Asian river systems reconstructed by trace element and Pb and Nd isotope variations in modern and ancient Red River-Song Hong sediments". *Geochemistry, Geophysics, Geosystems* 9(4), n/a–n/a. ISSN: 1525-2027. DOI: 10.1029/2007gc001867.

Defant, M. J. and M. S. Drummond (1990). "Derivation of some modern arc magmas by melting of young subducted lithosphere". *Nature* 347(6294), pages 662–665. DOI: 10.1038/347662a0.

Denton, G. H. and R. L. Armstrong (1969). "Miocene-Pliocene glaciations in southern Alaska". *American Journal of Science* 267(10), pages 1121–1142. DOI: 10.2475/ajs.267.10.1121.

Dickinson, W. R. (2008). "Impact of differential zircon fertility of granitoid basement rocks in North America on age populations of detrital zircons and implications for granite petrogenesis". *Earth and Planetary Science Letters* 275(1–2), pages 80–92. ISSN: 0012-821X. DOI: 10.1016/j.epsl.2008.08.003.

Engebretson, D. C., A. Cox, and R. G. Gordon (1985). *Relative Motions Between Oceanic and Continental Plates in the Pacific Basin*. DOI: 10.1130/spe206-p1.

Enkelmann, E. and T. A. Ehlers (2015). "Evaluation of detrital thermochronology for quantification of glacial catchment denudation and sediment mixing". *Chemical Geology* 411, pages 299–309. DOI: 10.1016/j.chemgeo.2015.07.018.

Gehrels, G. E. (2000). "Introduction to detrital zircon studies of Paleozoic and Triassic strata in western Nevada and northern California". *Paleozoic and Triassic paleogeography and tectonics of western Nevada and Northern California*. Edited by M. J. Soreghan and G. E. Gehrels. Geological Society of America. DOI: 10.1130/0-8137-2347-7.1.

– (2012). "Detrital Zircon U-Pb Geochronology: Current Methods and New Opportunities". *Tectonics of Sedimentary Basins: Recent Advances*. Edited by C. Busby and A. Azor. John Wiley Sons, Ltd, pages 45–62. ISBN: 9781444347166. DOI: 10.1002/9781444347166.ch2.

Grabowski, D. M., E. Enkelmann, and T. A. Ehlers (2013). "Spatial extent of rapid denudation in the glaciated St. Elias syntaxis region, SE Alaska". *Journal of Geophysical Research: Earth Surface* 118(3), pages 1921–1938. ISSN: 2169-9003. DOI: 10.1002/jgrf.20136.

Irvine, T. N. and W. R. A. Baragar (1971). "A Guide to the Chemical Classification of the Common Volcanic Rocks". *Canadian Journal of Earth Sciences* 8(5), pages 523–548. DOI: 10.1139/e71-055.

Keast, R. T., M. E. Brueseke, J. M. Trop, S. E. Berkelhammer, and J. Benowitz (2016). "Volcanic stratigraphy of the 2.4 Ma Euchre Mountain volcano, Wrangell Arc, Alaska (U.S.A.)" *Geological Society of America Abstracts with Programs*. Geological Society of America.

Le Bas, M. J., R. W. Le Maitre, A. Streckeisen, and B. Zanettin (1986). "A Chemical Classification of Volcanic Rocks Based on the Total Alkali-Silica Diagram". *Journal of Petrology* 27(3), pages 745–750. DOI: 10.1093/petrology/27.3.745.

Le Maitre, R. W. (1976). "The Chemical Variability of some Common Igneous Rocks". *Journal of Petrology* 17(4), pages 589–598. DOI: 10.1093/petrology/17.4.589.

Licht, K. J. and S. R. Hemming (2017). "Analysis of Antarctic glacigenic sediment provenance through geochemical and petrologic applications". *Quaternary Science Reviews* 164, pages 1–24. ISSN: 0277-3791. DOI: 10.1016/j.quascirev.2017.03.009.

MacKevett Jr, E. M. (1976). "Geologic map of the McCarthy Quadrangle, Alaska". *U.S. Geological Survey Miscellaneous Investigations Series Map 1032*. DOI: 10.3133/mf773a. [scale 1:250,000].

Malkowski, M. A., G. R. Sharman, S. A. Johnstone, M. J. Grove, D. L. Kimbrough, and S. A. Graham (2019). "Dilution and propagation of provenance trends in sand and mud: Geochemistry and detrital zircon geochronology of modern sediment from central California (U.S.A.)" *American Journal of Science* 319(10), pages 846–902. ISSN: 1945-452X. DOI: 10.2475/10.2019.02.

Malusà, M. G., A. Resentini, and E. Garzanti (2016). "Hydraulic sorting and mineral fertility bias in detrital geochronology". *Gondwana Research* 31, pages 1–19. ISSN: 1342-937X. DOI: 10.1016/j.gr.2015.09.002.

Mann, M. E., G. A. Abers, K. A. Daly, and D. H. Christensen (2022). "Subduction of an Oceanic Plateau Across South-central Alaska: Scattered-Wave Imaging". *Journal of Geophysical Research: Solid Earth* 127(1). DOI: 10.1029/2021jb022697.

Mertzman, S. A. (2000). "K-Ar results from the southern Oregon-northern California Cascade Range". *Oregon Geology* 62(4), pages 99–122.

– (2015). *XRF laboratory: overview and analytical procedures*. URL: https://www.fandm.edu/earth-environment/laboratory-facilities/instrument-use-and-instructions (visited on 02/27/2023).

Morter, B. K. (2017). "Understanding the history of a volcanic arc: Linking geochemistry of Cenozoic volcanic cobbles from the Wrangell arc, Alaska, to upper plate and subducting slab tectonic processes". Master's thesis. Kansas State University.

Nye, C. J. (1983). "Petrology and geochemistry of Okmok and Wrangell volcanoes, Alaska". PhD thesis. University of California, Santa Cruz.

Pavlis, G. L., M. A. Bauer, J. L. Elliott, P. Koons, T. L. Pavlis, N. Ruppert, K. M. Ward, and L. L. Worthington (2019). "A unified three-dimensional model of the lithospheric structure at the subduction corner in southeast Alaska: Summary results from STEEP". *Geosphere* 15(2), pages 382–406. ISSN: 1553-040X. DOI: 10.1130/ges01488.1.

Plafker, G. and H. C. Berg (1994). "Overview of the geology and tectonic evolution of Alaska". *The Geology of Alaska*. Edited by G. Plafker and H. C. Berg. Geological Society of America, pages 989–1021. DOI: 10.1130/dnag-gna-g1.989.

Preece, S. J. and W. K. Hart (2004). "Geochemical variations in the <5 Ma Wrangell Volcanic Field, Alaska: implications for the magmatic and tectonic development of a complex continental arc system". *Tectonophysics* 392(1–4), pages 165–191. ISSN: 0040-1951. DOI: 10.1016/j.tecto.2004.04.011.

Preece, S. J., R. G. McGimsey, J. A. Westgate, N. J. G. Pearce, W. K. Hart, and W. T. Perkins (2014). "Chemical complexity and source of the White River Ash, Alaska and Yukon". *Geosphere* 10(5), pages 1020–1042. ISSN: 1553-040X. DOI: 10.1130/ges00953.1.

Richter, D. H., C. C. Preller, K. A. Labay, and N. B. Shew (2006). "Geologic Map of the Wrangell-Saint Elias National Park and Preserve, Alaska". [Scientific Investigations Map 2877].

Richter, D. H., D. S. Rosenkrans, and M. J. Steigerwald (1995). "Guide to the volcanoes of the western Wrangell Mountains, Alaska; Wrangell-St. Elias National Park and Preserve". DOI: 10.3133/b2072.

Richter, D. H., J. G. Smith, M. A. Lanphere, G. B. Dalrymple, B. L. Reed, and N. Shew (1990). "Age and progression of volcanism, Wrangell volcanic field, Alaska". *Bulletin of Volcanology* 53(1), pages 29–44. DOI: 10.1007/bf00680318.

Sajona, F. G., R. C. Maury, H. Bellon, J. Cotten, M. J. Defant, and M. Pubellier (1993). "Initiation of subduction and the generation of slab melts in western and eastern Mindanao, Philippines". *Geology* 21(11), page 1007. DOI: 10.1130/0091-7613(1993)021<1007:iosatg>2.3.co;2.

Satkoski, A. M., B. H. Wilkinson, J. Hietpas, and S. D. Samson (2013). "Likeness among detrital zircon populations–An approach to the comparison of age frequency data in time and space". *Geological Society of America Bulletin* 125(11–12), pages 1783–1799. ISSN: 1943-2674. DOI: 10.1130/b30888.1.

Saylor, J. E. and K. E. Sundell (2016). "Quantifying comparison of large detrital geochronology data sets". *Geosphere* 12(1), pages 203–220. ISSN: 1553-040X. DOI: 10.1130/ges01237.1.

Skulski, T., D. Francis, and J. Ludden (1991). "Arc-transform magmatism in the Wrangell volcanic belt". *Geology* 19(1), page 11. DOI: 10.1130/0091-7613(1991)019<0011:atmitw>2.3.co;2.

– (1992). "Volcanism in an arc-transform transition zone: the stratigraphy of the St. Clare Creek volcanic field, Wrangell volcanic belt, Yukon, Canada". *Canadian Journal of Earth Sciences* 29(3), pages 446–461. DOI: 10.1139/e92-039.

Spencer, C. J., C. L. Kirkland, and N. M. W. Roberts (2018). "Implications of erosion and bedrock composition on zircon fertility: Examples from South America and Western Australia". *Terra Nova* 30(4), pages 289–295. ISSN: 0954-4879. DOI: 10.1111/ter.12338.

Trop, J. M., J. A. Benowitz, C. S. Kirby, and M. E. Brueseke (2022). "Geochronology of the Wrangell Arc: Spatial-temporal evolution of slab-edge magmatism along a flat-slab, subduction-transform transition, Alaska-Yukon". *Geosphere* 18(1), pages 19–48. DOI: 10.1130/ges02417.1.

Trop, J. M., W. K. Hart, D. Snyder, and B. Idleman (2012). "Miocene basin development and volcanism along a strike-slip to flat-slab subduction transition: Stratigraphy, geochemistry, and geochronology of the central Wrangell volcanic belt, Yakutat–North America collision zone". *Geosphere* 8(4), pages 805–834. ISSN: 1553-040X. DOI: 10.1130/ges00762.1.

VanderLeest, R. A., J. C. Fosdick, J. S. Leonard, and L. E. Morgan (2020). "Detrital record of the late Oligocene – early Miocene mafic volcanic arc in the southern Patagonian Andes (~51°S) from single-clast geochronology and trace element geochemistry". *Journal of Geodynamics* 138, page 101751. DOI: 10.1016/j.jog.2020.101751.

Waldien, T. S., S. M. Roeske, and J. A. Benowitz (2021). "Tectonic Underplating and Dismemberment of the Maclaren-Kluane Schist Records Late Cretaceous Terrane Accretion Polarity and 480 km of Post-52 Ma Dextral Displacement on the Denali Fault". *Tectonics* 40(10). ISSN: 1944-9194. DOI: 10.1029/2020tc006677.

Waldien, T. S., S. M. Roeske, J. A. Benowitz, W. K. Allen, K. D. Ridgway, and P. B. O'Sullivan (2018). "Late Miocene to Quaternary evolution of the McCallum Creek thrust system, Alaska: Insights for range-boundary thrusts in transpressional orogens". *Geosphere* 14(6), pages 2379–2406. ISSN: 1553-040X. DOI: 10.1130/ges01676.1.

Wells, R., D. Bukry, R. Friedman, D. Pyle, R. Duncan, P. Haeussler, and J. Wooden (2014). "Geologic history of Siletzia, a large igneous province in the Oregon and Washington Coast Range: Correlation to the geomagnetic polarity time scale and implications for a long-lived Yellowstone hotspot". *Geosphere* 10(4), pages 692–719. ISSN: 1553-040X. DOI: 10.1130/ges01018.1.

Worthington, L. L., H. J. A. Van Avendonk, S. P. S. Gulick, G. L. Christeson, and T. L. Pavlis (2012). "Crustal structure of the Yakutat terrane and the evolution of subduction and collision in southern Alaska". *Journal of Geophysical Research: Solid Earth* 117(B1), n/a–n/a. ISSN: 0148-0227. DOI: 10.1029/2011jb008493.

Zhang, L., S. Li, and Q. Zhao (2019). "A review of research on adakites". *International Geology Review* 63(1), pages 47–64. DOI: 10.1080/00206814.2019.1702592.